J|A|C|S
ARTICLES
Published on Web 01/09/2003

Heavy Atom Isotope Effects on the Reaction Catalyzed by the Oxalate Decarboxylase from *Bacillus subtilis*

Laurie A. Reinhardt,[†] Drazenka Svedruzic,[‡] Christopher H. Chang,[‡,§] W. Wallace Cleland,*[,†] and Nigel G. J. Richards*[,‡]

Contribution from the Department of Chemistry, University of Florida, Gainesville, Florida 32611-7200, and the Institute for Enzyme Research and Department of Biochemistry, University of Wisconsin—Madison, 1710 University Avenue, Madison, Wisconsin 53726

Received September 25, 2002; E-mail: cleland@enzyme.wisc.edu, richards@qtp.ufl.edu.

Abstract: Oxalate decarboxylase (OxDC) catalyzes a remarkable transformation in which the C−C bond in oxalate is cleaved to give carbon dioxide and formate. Like the native OxDC isolated from *Aspergillus niger*, the recombinant, bacterial OxDC from *Bacillus subtilis* contains Mn(II) in its resting state and requires catalytic dioxygen for activity. The most likely mechanism for OxDC-catalyzed C−C bond cleavage involves the participation of free radical intermediates, although this hypothesis remains to be unequivocally demonstrated. Efforts to delineate the catalytic mechanism have been placed on a firm foundation by the high-resolution crystal structure of recombinant, wild type *B. subtilis* OxDC (Anand et al., *Biochemistry* 2002, *41*, 7659−7669). We now report the results of heavy-atom kinetic isotope effect measurements for the OxDC-catalyzed decarboxylation of oxalate, in what appear to be the first detailed studies of the mechanism employed by OxDC. At pH 4.2, the OxDC-catalyzed formation of formate and CO_2 have normal ^{13}C isotope effects of 1.5% ± 0.1% and 0.5% ± 0.1%, respectively, while the ^{18}O isotope effect on the formation of formate is 1.1% ± 0.2% normal. Similarly at pH 5.7, the production of formate and CO_2 exhibits normal ^{13}C isotope effects of 1.9% ± 0.1% and 0.8% ± 0.1%, respectively, and the ^{18}O isotope effect on the formation of formate is 1.0% ± 0.2% normal. The ^{18}O isotope effect on the formation of CO_2, however, 0.7% ± 0.2%, is inverse at pH 5.7. These results are consistent with a multistep model in which a reversible, proton-coupled, electron transfer from bound oxalate to the Mn-enzyme gives an oxalate radical, which decarboxylates to yield a formate radical anion. Subsequent reduction and protonation of this intermediate then gives formate.

Introduction

Oxalic acid, a compound that is toxic to almost all organisms,[1] plays several important roles in both fungal growth and metabolism[2] and the biological mechanisms underlying fungal pathogenesis.[3] A number of enzymes have evolved in plants (oxalate oxidase),[4] fungi (oxalate decarboxylase),[5] and bacteria (oxalyl-CoA decarboxylase)[6] to remove oxalate from the environment. Of these, oxalate decarboxylase (OxDC) catalyzes a remarkable transformation in which the C−C bond in oxalate is cleaved to give carbon dioxide and formate (Scheme 1).

Oxalate decarboxylases were first isolated from basidiomycete fungi[5] and have subsequently been identified in several species of filamentous fungi, including *Myrothecium verrucari*,[7] certain strains of *Aspergillus niger*,[8] *Flammulina velutipes*,[9] and the common button mushroom *Agaricus bisporus*.[10] This enzyme can also be induced in the white-rot fungus *Coriolus versicolor*.[11] The purification of native OxDC from fungal sources,

Scheme 1. Enzyme-Catalyzed Reactions Employed in the Degradation of Oxalate

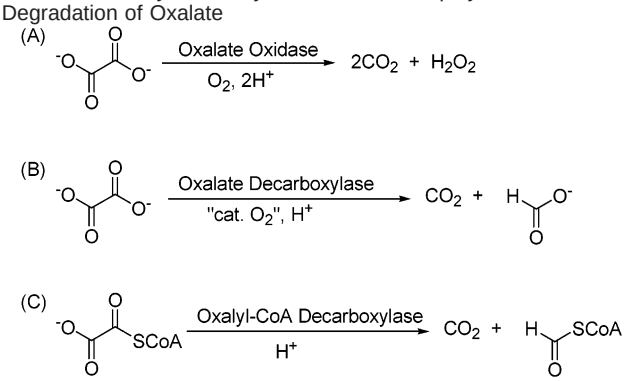

[†] University of Wisconsin—Madison.
[‡] University of Florida.
[§] Recipient of an NIH postdoctoral fellowship (DK61193).

(1) Hodgkinson, A. *Oxalic Acid in Biology and Medicine*; Academic Press: London, 1977.
(2) Dutton, M. V.; Evans, C. S. *Can. J. Microbiol.* **1996**, *42*, 881−895.
(3) Landry, M. L. M.; Parkins, C. W. *Mod. Pathol.* **1993**, *6*, 493−496.
(4) Kotsira, V. P.; Clonis, Y. D. *Arch. Biochem. Biophys.* **1997**, *340*, 239−249.
(5) Shimazono, H. *J. Biochem. (Tokyo)* **1955**, *42*, 321−340.
(6) Quayle, J. R. *Biochem. J.* **1963**, *87*, 368−373.
(7) Lillehoj, E. B.; Smith, F. G. *Arch. Biochem. Biophys.* **1965**, *109*, 216−220.
(8) Emiliani, E.; Bekes, P. *Arch. Biochem. Biophys.* **1964**, *105*, 488−493.
(9) Mehta, A.; Datta, A. *J. Biol. Chem.* **1991**, *266*, 23548−23553.
(10) Shimazono, H.; Haiyashi, O. *J. Biol. Chem.* **1957**, *227*, 151−159.

10.1021/ja0286977 CCC: $25.00

however, yields relatively small amounts of material, which has hampered a number of previous efforts to determine the mechanism employed by this interesting enzyme.[12] The demonstration that the *yvrk* gene in *Bacillus subtilis* encodes a bacterial OxDC[13] that can be obtained in large quantities by expression in *Escherichia coli*,[14] therefore represents a watershed in studying the biochemical properties of OxDC. In addition, efforts to delineate the catalytic mechanism have been placed on a firm foundation by the high-resolution crystal structure of recombinant, wild-type *B. subtilis* OxDC,[15] which has confirmed the hypothesis that OxDC is a member of the cupin superfamily[16,17] and is evolutionarily related to oxalate oxidase.[18,19]

The OxDC crystal structure confirms that the enzyme contains two Mn-binding sites,[15] consistent with proposals based on sequence alignment[16] and metal analysis studies, and rules out the involvement of redox-active cofactors[20,21] in the catalytic mechanism. Although three histidine residues and a glutamic acid side chain coordinate Mn in both metal sites, there are significant structural differences that suggest catalysis takes place in only the C-terminal domain.[15] In light of the demonstrated dependence of OxDC activity on a catalytic amount of dioxygen,[12,14,22] it has been proposed that bound Mn undergoes oxidation to give a species capable of abstracting an electron to form an oxalate radical that then undergoes decarboxylation to yield a formate radical anion.[15] Indirect support for the involvement of formate radical during enzyme-catalyzed C−C bond cleavage in substrate oxalate has been obtained in electron paramagnetic resonance (EPR) spin-trapping experiments involving recombinant, wild-type oxalate oxidase (OxOx).[19] Although it has also been speculated that Mn(III) and Mn(IV) are the redox-active forms of the metal in OxDC during catalysis,[15] this claim remains to be verified. Equally, the intermediacy of a protein-based radical[23] cannot be ruled out on the basis of current biochemical[13,14] and structural information[15] on *B. subtilis* OxDC. The location of a single cysteine residue at the C-terminus of the bacterial enzyme, however, argues against the involvement of a thiyl radical as observed in pyruvate−formate lyase.[24]

We now report the results of heavy-atom kinetic isotope effect (KIE) measurements[25] for the OxDC-catalyzed decarboxylation of oxalate. These experiments represent the first detailed measurements of the catalytic mechanism employed by this enzyme and are consistent with a multistep model in which a reversible, proton-coupled[26,27] electron-transfer step from bound oxalate to the Mn-enzyme complex precedes a faster, heterolytic C−C bond cleavage step.

Experimental Section

Expression and Purification of Recombinant *B. subtilis* OxDC. The *yvrk* gene from *B. subtilis* 168[28] was PCR-amplified with the high-fidelity *Pfu* polymerase. PCR primers contained restriction site sequences for *Nde*I at the N-terminal methionine (5′ primer, sequence 5′-GGAGGAAACATCATATGAAAAAACAAAATG-3′) and *Bam*HI after the *yvrk* termination codon (3′ primer, sequence 5′-GCGGCAGGATCCTTATTTACTGCATTTC-3′). These primers were designed such that the *yvrk* coding sequence would be in-frame with the T7 control elements that are part of the pET-9a expression vector (Stratagene). *B. subtilis* 168 genomic DNA was purified from an overnight culture (5 mL) with a Genomic DNA Miniprep kit (Qiagen). The *yvrk* sequence was amplified for 31 cycles (95 °C denaturation, 30 s; 45 °C annealing, 30 s; 74 °C extension, 2 min), and the resulting DNA was digested with *Nde*I and *Bam*HI before being ligated into pET-9a that had also been digested with these restriction enzymes. Competent JM109 cells were transformed with the ligation mixture and with pET-9a as a control, and transformants selected on Luria−Bertani broth (LB) containing 30 μg/mL kanamycin (LBK). The resulting colonies were screened by *Nde*I−*Bam*HI digestion to confirm the presence of an 1153 bp insert, and the cloned gene was sequenced by standard methods (Interdisciplinary Center for Biotechnology, University of Florida). A plasmid produced from *yvrk*:pET-9a/JM109 by standard alkaline lysis miniprep was used to transform the expression strain BL21(DE3), and the expression of the *yvrk*-encoded protein was accomplished by inoculating 0.5 L of LBK with *yvrk*:pET-9a/BL21-(DE3). The cells were grown at 37 °C and shaken until the cultures reached an absorbance (A_{600}) value of 1.7, at which time the bacteria were heat-shocked at 42 °C for 18 min before the addition of isopropyl thiogalactoside (IPTG) and $MnCl_2$ to final concentrations of 1 and 5 mM, respectively. The cells were harvested after 4 h by centrifugation (5000 rpm, 15 min, 4 °C), and the pellets were resuspended in 50 mL lysis buffer (50 mM Tris·HCl, pH 7, containing 10 μM $MnCl_2$) before being sonicated for 30 s. After sonication, lysis pellets were separated from the crude extract by centrifugation (8000 rpm, 20 min, 4 °C) and resuspended in 50 mL of extraction buffer containing 1 M sodium chloride, 0.1% Triton X-100, and 10 mM 2-mercaptoethanol. The mixture was stirred overnight at room temperature. Cell debris was

(11) Kathiara, M.; Wood, D. A.; Evans, C. S. *Mycol. Res.* **2000**, *104*, 345−350.
(12) Emiliani, E.; Riera, B. *Biochim. Biophys. Acta* **1968**, *167*, 414−421.
(13) Tanner, A.; Bornemann, S. *J. Bacteriol.* **2000**, *182*, 5271−5273.
(14) Tanner, A.; Bowater, L.; Fairhurst, S. A.; Bornemann, S. *J. Biol. Chem.* **2001**, *276*, 14627−14634.
(15) Anand, R.; Dorrestein, P. C.; Kinsland, C.; Begley, T. P.; Ealick, S. E. *Biochemistry* **2002**, *41*, 7659−7669.
(16) Dunwell, J. M.; Khuri, S.; Gane, P. J. *Microbiol. Mol. Biol. Rev.* **2000**, *64*, 153−179.
(17) Clissold, P. M.; Ponting, C. P. *Trends Biochem. Sci.* **2001**, *26*, 7−9.
(18) Woo, E.-J.; Dunwell, J. M.; Goodenough, P. W.; Marvier, A. C.; Pickersgill, R. W. *Nat. Struct. Biol.* **2000**, *7*, 1036−1040.
(19) Whittaker, M. M.; Whittaker, J. W. *J. Biol. Inorg. Chem.* **2002**, *7*, 136−145.
(20) Klinman, J. P.; Mu, D. *Annu. Rev. Biochem.* **1994**, *63*, 299−344.
(21) Halcrow, M. A. *Angew. Chem., Int. Ed.* **2001**, *40*, 346−349.
(22) Kesarwani, M.; Azam, M.; Natarajan, K.; Mehta, A.; Datta, A. *J. Biol. Chem.* **2000**, *275*, 7230−7238.
(23) Stubbe, J. A.; van der Donk, W. A. *Chem. Rev.* **1998**, *98*, 705−782.
(24) (a) Becker, A.; Fritz-Wolf, K.; Kabsch, W.; Knappe, J.; Schultz, S.; Wagner, A. F. V. *Nat. Struct. Biol.* **1999**, *6*, 969−975. (b) Himo, F.; Eriksson, L. A. *J. Am. Chem. Soc.* **1998**, *120*, 11449−11455.
(25) (a) O'Leary, M. H. *Annu. Rev. Biochem.* **1989**, *58*, 377−401. (b) O'Leary, M. H. *Methods Enzymol.* **1980**, *64*, 83−104. (c) Klinman, J. P. *Adv. Enzymol. Relat. Areas Mol. Biol.* **1978**, *46*, 415−494.
(26) Su, Q. J.; Klinman, J. P. *Biochemistry* **1964**, *37*, 12513−12525.
(27) Klinman, J. P. *J. Biol. Inorg. Chem.* **2001**, *6*, 1−13.
(28) Kunst, F.; Ogasawara, N.; Moszer, I.; Albertini, A. M.; Alloni, G.; Azevedo, V.; Bertero, M. G.; Bessieres, P.; Bolotin, A.; Borchert, S.; Borriss, R.; Boursier, L.; Brans, A.; Braun, M.; Brignell, S. C.; Bron, S.; Brouillet, S.; Bruschi, C. V.; Caldwell, B.; Capuano, V.; Carter, N. M.; Choi, S. K.; Codani, J. J.; Connerton, I. F.; Cummings, N. J.; Daniel, R. A.; Denizot, F.; Devine, K. M.; Dusterhoft, A.; Ehrlich, S. D.; Emmerson, P. T.; Entian, K. D.; Errington, J.; Fabret, C.; Ferrari, E.; Foulger, D.; Fritz, C.; Fujita, M.; Fujita, Y.; Fuma, S.; Galizzi, A.; Galleron, N.; Ghim, S. Y.; Glaser, P.; Goffeau, A.; Golightly, E. J.; Grandi, G.; Guiseppi, G.; Guy, B. J.; Haga, K.; Haiech, J.; Harwood, C. R.; Henaut, A.; Hilbert, H.; Holsappel, S.; Hosono, S.; Hullo, M. F.; Itaya, M.; Jones, L.; Joris, B.; Karamata, D.; Kasahara, Y.; Klaerr-Blanchard, M.; Klein, C.; Kobayashi, Y.; Koetter, P.; Koningstein, G.; Krogh, S.; Kumano, M.; Kurita, K.; Lapidus, A.; Lardinois, S.; Lauber, J.; Lazarevic, V.; Lee, S. M.; Levine, A.; Liu, H.; Masuda, S.; Mauel, C.; Medigue, C.; Medina, N.; Mellado, R. P.; Mizuno, M.; Moestl, D.; Nakai, S.; Noback, M.; Noone, D.; O'Reilly, M.; Ogawa, K.; Ogiwara, A.; Oudega, B.; Park, S. H.; Parro, V.; Pohl, T. M.; Portetelle, D.; Porwollik, S.; Prescott, A. M.; Presecan, E.; Pujic, P.; Purnelle, B.; Rapoport, G.; Rey, M.; Reynolds, S.; Rieger, M.; Rivolta, C.; Rocha, E.; Roche, B.; Rose, M.; Sadaie, Y.; Sato, T.; Scanlan, E.; Schleich, S.; Schroeter, R.; Scoffone, F.; Sekiguchi, J.; Sekowska, A.; Serror, S. J.; Serror, P.; Shin, B. S.; Soldo, B.; Sorokin, A.; Tacconi, E.; Takagi, T.; Takahashi, H.; Takemaru, K.; Takeuchi, M.; Tamakoshi, A.; Tanaka, T.; Terpstra, P.; Tognoni, A.; Tosato, V.; Uchiyama, S.; Vandenbol, M.; Vannier, F.; Vassarotti, A.; Viari, A.; Wambutt, R.; Wedler, E.; Wedler, H.; Weitzenegger, T.; Winters, P.; Wipat, A.; Yamamoto, H.; Yamane, K.; Yasumoto, K.; Yata, K.; Yoshida, K.; Yoshikawa, H. F.; Zumstein, E.; Yoshikawa, H.; Danchin, A. *Nature* **1997**, *390*, 249−256.

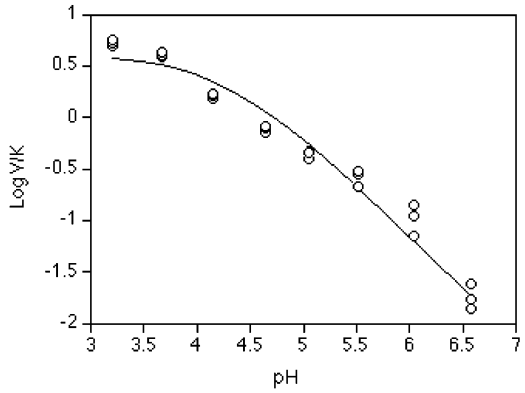

Figure 1. pH dependence of $V/K_{oxalate}$ for recombinant *B. subtilis* OxDC. The enzyme is not stable below pH 2.8 (Svedruzic, unpublished results). The experimental data (○) were fitted to log y = log $[C/(1 + K/H)]$,[30] which gave a pK_a value of 4.2 ± 0.1.

removed by centrifugation and the supernatant was combined with the crude extract. This solution (100 mL) was diluted 10-fold before it was applied to a 2.5 × 30 cm DEAE-Sepharose Fast Flow (Sigma) column. The column was washed with imidazole hydrochloride buffer (50 mM, pH 7.0, containing 10 μM $MnCl_2$) and developed with a 500 mL NaCl gradient (0 → 1 M). Fractions were collected and assayed for their ability to oxidize *o*-phenylenediamine in a side reaction catalyzed by OxDC, and those fractions exhibiting activity were pooled before the addition of solid $(NH_4)_2SO_4$ to a final concentration of 1.7 M. The precipitate was removed by centrifugation (8000 rpm, 30 min, 4 °C), and the supernatant was loaded onto a phenyl-Sepharose Hi-Performance (Amersham Pharmacia Biotech) column. The column was washed with imidazole hydrochloride buffer (50 mM, pH 7.0, containing 10 μM $MnCl_2$) and developed with a 500 mL $(NH_4)_2SO_4$ gradient (1.7 → 0 M). The fractions were pooled as for the DEAE column and diluted 15-fold before they were loaded onto a Q-Sepharose Hi-Performance (Amersham Pharmacia Biotech) column. The protein was eluted with an imidazole hydrochloride buffer (50 mM, pH 7.0, containing 10 μM $MnCl_2$) and a 500 mL NaCl gradient (0 → 1 M) as for the DEAE column. The purified protein was then concentrated by ultrafiltration (Amicon) to a volume of 10 mL and dialyzed for 4 h against 1 L of storage buffer (20 mM hexamethylenetetramine hydrochloride, pH 6, containing 0.5 M NaCl). The resulting solution was again concentrated, and aliquots were flash-frozen in liquid N_2 and stored at −80 °C. This procedure gave purified OxDC in yields of up to 30 mg/L with a specific activity of approximately 50 IU/mg.

OxDC Assays. Assay mixtures consisted of 50 mM buffer, 0.2% Triton X-100, 0.5 mM *o*-phenylenediamine, 1−50 mM potassium oxalate, and 2 μM enzyme subunits (100 μL total volume). Turnover was initiated by addition of substrate. Mixtures were incubated at ambient temperature (21−22 °C), and then the reaction was quenched by addition of 10 μL of 1 N NaOH. The amount of formate produced in an aliquot (50 μL) taken from the OxDC-catalyzed reaction mixture was determined by a formate dehydrogenase (FDH) assay[29] consisting of 50 mM potassium phosphate, pH 7.8, 0.9 mM NAD^+, and 0.4 IU of FDH (1 mL final volume). The absorbance at 340 nm was measured after overnight incubation at 37 °C, and formate was quantitated by comparison to a standard curve generated by spiking protein-free OxDC assays with known amounts of sodium formate. Measurements at specific substrate concentrations were performed in triplicate, and the initial rate data were analyzed to obtain the values of V and V/K by curve-fitting by standard computer-based methods.[30] The initial rate of formate production was expressed in millimoles per liter per minute.

The pH dependence of V/K (Figure 1) for *B. subtilis* OxDC-catalyzed oxalate degradation was measured in the following series of buffers: pH 2.8 and 3.2, glycine; pH 3.8, 4.2, 4.7, and 5.2, acetate; pH 5.7, 6.2, and 6.7, MES; pH 7, BES; and pH 7.7 and 8.2, EPPS.

Isotope Effect Nomenclature. The nomenclature used in this work is that due to Northrop,[31] in which $^{13}(V/K)$ represents the ratio of V/K for the ^{12}C-containing species relative to the ^{13}C-containing species, and $^{18}(V/K)$ is a similar ratio for ^{16}O and ^{18}O.

^{13}C and ^{18}O Isotope Effect Determinations. The primary ^{13}C and secondary ^{18}O isotope effects for the OxDC-catalyzed decarboxylation reaction were measured by isotope ratio mass spectrometric analysis of CO_2(g),[25b] by the internal competition method, and hence these isotope effects represent the effects of isotopic substitution on $V/K_{oxalate}$. Their values are therefore associated only with steps up to, and including, the first irreversible step in the mechanism. Natural-abundance levels of isotopic label in the carbon and oxygen atoms of oxalate were used in these experiments. The analyses to determine the isotopic ratios (R values) were performed on CO_2(g), which was either isolated directly from OxDC-catalyzed partial conversion of oxalate (R_{CO_2}) or produced by oxidation reactions of initial oxalate (R_0), formate ($R_{formate}$), and oxalate (R_s) from residual substrate after partial reaction with I_2 in anhydrous DMSO.[32]

In these isotope effect determinations, the enzymatic reactions were performed by incubation of OxDC with oxalate (27−43 mM) and *o*-phenylenediamine (0.5 mM) at 22 °C in either 0.1 M 1,4-bis-(2-hydroxyethyl)piperazine, pH 4.2, or piperazine, pH 5.7 (920 μL total volume). All gases were passed over Ascarite to remove CO_2(g) prior to use. Buffer solutions and aqueous solutions of oxalate/*o*-phenylenediamine were sparged beforehand with O_2(g) and N_2(g) (which had been passed through 1 N aqueous H_2SO_4 in addition to being treated with Ascarite), respectively. The presence of oxygen is required for OxDC activity, precluding the sparging of both solutions with only N_2(g). After addition of buffer to the substrate solution, sufficient OxDC was added to yield reaction times of between 7 min and 2 h. OxDC-catalyzed reactions were quenched by raising the solution pH to 7.5 with 1 N Tris-H_2SO_4, pH 7.5. The fraction of conversion, f, was determined by use of FDH and an oxalate detection kit (Sigma) to measure formate and remaining oxalate concentrations, respectively. CO_2(g) was collected during the OxDC-catalyzed reaction and purified as previously described.[25b] Oxalate and formate were separated on Bio-Rad AG-1 ion-exchange resin (1 × 4 cm) and eluted with aqueous H_2SO_4 (pH 2.5−2.7). The column fractions were monitored by the FDH and oxalate assays described above, and the desired fractions were pooled. HEPES (1 M, pH 7.0, 0.5 mL) was added to the fractions containing formate, while oxalate samples were neutralized with NaOH. After rotoevaporation to remove most of the H_2O, samples were again sparged with N_2(g) to remove any dissolved, atmospheric CO_2(g). After removal of residual water under vacuum (<1 Torr), these samples were placed on a vacuum line (<1 Torr) and heated at 70 °C overnight. An anhydrous solution of I_2 (0.15−0.2 g) dissolved in DMSO (2 mL) was then syringed into the dried samples, which were residing on the vacuum line, and the CO_2(g) evolved in the oxidation reaction was distilled through two pentane/N_2(l) traps before being collected in a N_2(l) trap. CO_2(g) was further distilled from a pentane/N_2(l) trap into a collection flask cooled with N_2(l). Whereas formate oxidation produces 1 equiv of CO_2(g), each molecule of oxalate gives 2 equiv of CO_2(g). Control samples in which the reaction was quenched before the addition of OxDC did not contain detectable amounts of CO_2(g). Experiments with ^{18}O-enriched water (Isotec) were performed in a manner similar to that described above except that the reaction solutions contained 5% $H_2{}^{18}O$.

(29) Schutte, H.; Flossdorf, J.; Sahm, H.; Kula, M. R. *Eur. J. Biochem.* **1976**, *62*, 151−160.
(30) Cleland, W. W. *Methods Enzymol.* **1979**, *63*, 103−138.
(31) Northrop, D. B. In *Isotope Effects on Enzyme-Catalyzed Reactions*; Cleland, W. W., O'Leary, M. H., Northrop, D. B., Eds.; University Park Press: Baltimore, MD, 1977; pp 122−148.
(32) Hermes, J. D.; Morrical, S. W.; O'Leary, M. H.; Cleland, W. W. *Biochemistry* **1984**, *23*, 5479−5488.

Table 1. ^{13}C and ^{18}O Isotope Effects on the Reaction Catalyzed by *B. subtilis* OxDC[a]

	$^{13}(V/K)$, %		$^{18}(V/K)$,[b] %	
pH (buffer)	CO_2	HCO_2^-	CO_2	HCO_2^-
4.2 (BHEP)	0.5 ± 0.1	1.5 ± 0.1	−0.2 ± 0.2	1.1 ± 0.2
5.7 (piperazine)	0.8 ± 0.1	1.9 ± 0.1	−0.7 ± 0.1	1.0 ± 0.1

[a] Values are reported for 27−43 mM oxalate at 22 °C. [b] Value is given per two oxygen atoms.

The isotopic ratios of each sample of CO_2(g) were measured on a Finnegan Mat spectrometer, and the following equation was used to determine the apparent isotope effect (app·IE):

$$\text{app·IE} = \frac{\ln(1-f)}{\ln\left[(1-f)\left(\frac{R_s}{R_0}\right)\right]} = \frac{\ln(1-f)}{\ln\left[1-f\left(\frac{R_p}{R_0}\right)\right]} \quad (1)$$

where R_s is the mass ratio of the isotope (^{13}C or ^{18}O) in residual oxalate at the fraction of reaction f, and R_0 is the value for the oxalate substrate before reaction. Similarly, R_{CO_2} and $R_{formate}$ are the cognate mass ratios in CO_2(g) or formate at f, respectively, and R_p is their average. The ^{13}C or ^{18}O isotope effects on the formation of CO_2 and formate were then calculated by use of eqs 2 and 3:

$$\text{isotope effect for formation of } CO_2 = \left[\frac{(1+x)}{2x}\right]\text{app·IE} \quad (2)$$

$$\text{isotope effect for formation of formate} = \left[\frac{(1+x)}{2}\right]\text{app·IE} \quad (3)$$

where x is the $R_{CO_2}/R_{formate}$ ratio. The ^{18}O mass ratio in the CO_2 product was determined by comparing the original R_0 value with that for R_s and $R_{formate}$. A complete derivation of eqs 2 and 3 is given in the Appendix.

Results and Discussion

pH Dependence of OxDC Activity. Both $V/K_{oxalate}$ (Figure 1) and V decreased as the pH of the reaction buffer was raised above 4. When the observed $V/K_{oxalate}$ values were multiplied by $(1 + K/H)$, where K is the second acid dissociation constant of oxalic acid (4.2)[33] and H is the hydrogen ion concentration, the resulting V/K values were essentially invariant with pH, suggesting that monoprotonated oxalate is the actual substrate for OxDC.

^{13}C Isotope Effects. The ^{13}C and ^{18}O isotope effects (IEs) were measured on the reaction catalyzed by OxDC at pH 4.2 and pH 5.7 (Table 1). For rate-limiting C−C cleavage reactions, normal ^{13}C IEs of 3−5% are typical. However, for the OxDC-catalyzed reaction the ^{13}C IE values for the CO_2 product (normal 0.5−0.8%) were lower than expected, indicating that C−C bond cleavage is not the major rate-limiting step. The observation that the ^{13}C KIE for formate production (normal 1.5−1.9%) is 3-fold larger than that for CO_2 is consistent with the presence of a different step that is slower than C−C bond cleavage. Moreover, the normal ^{13}C IEs observed are most likely due to a decrease in C−O bond order in this step. Given that the formation of CO_2 is most likely irreversible, the slower, reversible step precedes C−C bond cleavage to give this gaseous product. At pH 5.7, the chemical steps are somewhat more rate-limiting as compared to those at pH 4.2, as shown by the increase in the observed ^{13}C IEs. This difference is presumably the result of an external commitment at the higher solution pH (see below).

^{18}O Isotope Effects. As observed for the ^{13}C IE, the ^{18}O IE is normal (1.0−1.1%) for formation of formate (Table 1). In contrast, the ^{18}O IE for CO_2 production is inverse (−0.2% to −0.7%), consistent with the fact that the bond order for these oxygens increases from 1.5 in the substrate to 2 in the product. Similar measurements on decarboxylases, for which the chemistry step is rate-limiting, have given ^{18}O IE values of −0.4% to −0.5%.[34] In addition to the effects of changes in bond orders,^{18}O IEs can also be influenced by changes in protonation state. For example, the equilibrium ^{18}O IE for protonation of a carboxyl group has been shown to be 0.98.[35] Since the V/K profile (Figure 1) for OxDC suggests that monoprotonated oxalate is the substrate, the effects of protonation must be taken into account in deducing the chemistry of the enzyme-catalyzed reaction from the observed ^{18}O IE values.

A further complication in interpreting the experimental ^{18}O IEs values is the possibility that water attacks an intermediate in the OxDC-catalyzed reaction, resulting in the presence of oxygens in the residual substrate or products derived from the solvent. We therefore examined whether exchange of the solvent oxygens into formate or oxalate took place under the reaction conditions by incubating OxDC with substrate in a solution containing 5% $H_2{}^{18}O$. Only 0.2% of ^{18}O incorporation into both formate and oxalate was observed under these conditions, and no exchange was found in control reactions performed under identical conditions, with the exception that formate instead of OxDC was added at the start of the incubation. While ^{18}O exchange is therefore dependent on the presence of active OxDC, it occurs to a minimal extent, confirming the validity of our ^{18}O IE measurements.

Fractionation Factors of Oxalate and Its Radical. The BEBOVIB program[36] was used to estimate the ^{13}C and ^{18}O fractionation factors of oxalate relative to CO_2 gas, using a force field that closely reproduced the experimental IR and Raman frequencies of oxalate.[37] Assuming C−O bond orders of 1.5 in oxalate, the ^{13}C and ^{18}O fractionation factors vs CO_2 were computed to be 0.9838 and 0.9674, respectively, which are reasonable numbers. We then systematically decreased the C−O bond order in one end of oxalate to a value of 1.0, while maintaining the C−O bond order at 1.5 in the other carboxylate group. These calculations showed that reducing the C−O bond order lowered the ^{13}C and ^{18}O fractionation factors in a linear fashion to 0.9537 and 0.9465, respectively (Figure 2). In a similar manner, we demonstrated that the ^{18}O fractionation factor in the other carboxylate was almost unchanged and the ^{13}C value decreased slightly to 0.9828. These calculated values were subsequently employed in estimating the actual bond orders in the oxalate radical (see below).

(33) Speakman, J. C. *J. Chem. Soc.* **1940**, 855−859.
(34) (a) Headley, G. W.; O'Leary, M. H. *J. Am. Chem. Soc.* **1990**, *112*, 1894−1896. (b) Waldrop, G. L.; Braxton, B. F.; Urbauer, J. L.; Cleland, W. W.; Kiick, D. M. *Biochemistry* **1994**, *33*, 5262−5267.
(35) Tanaka, N.; Araki, M. *J. Am. Chem. Soc.* **1985**, *107*, 7780−7781.
(36) (a) Sims, L. B.; Lewis, D. E. In *Isotopes in Organic Chemistry, Vol. 6: Isotopic Effects. Recent Developments in Theory and Experiment*; Buncel, E., Lee, C. C., Eds.; Elsevier: Amsterdam, 1984; pp 161−259. (b) Berti, P. J. *Methods Enzymol.* **1999**, *308*, 355−397.
(37) Ito, K.; Bernstein, H. J. *Can. J. Chem.* **1956**, *34*, 170−178.

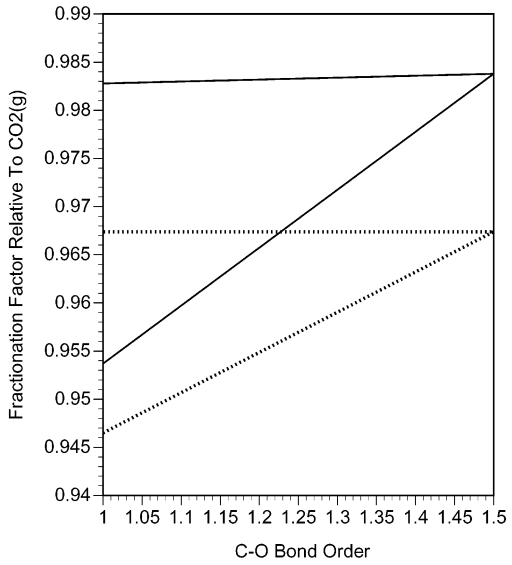

Figure 2. Fractionation factors of oxalate carbons and oxygens as a function of C−O bond order. The sloping lines are for the carboxyl whose C−O bond order is varied, while the nearly horizontal lines are for the other carboxyl group where the bond order remains 1.5. (—) ^{13}C; (···) ^{18}O.

Analysis of the Observed $^{13}(V/K)$ and $^{18}(V/K)$ Isotope Effects. The observed ^{13}C and ^{18}O isotope effects rule out any mechanism for the OxDC-catalyzed breakdown of oxalate that does not include an isotope-sensitive, reversible step prior to decarboxylation. A minimal kinetic mechanism for the enzyme can therefore be written as

$$\text{E} + \text{oxalate} \underset{k_2}{\overset{k_1}{\rightleftharpoons}} \text{E-oxalate} \underset{k_4}{\overset{k_3}{\rightleftharpoons}} \text{E-oxalate}\bullet \xrightarrow{k_5} \text{E-formate}\bullet + \text{CO}_2 \quad (4)$$

The remaining steps to yield formate and the free enzyme must then involve protonation and reduction of the formate radical anion. We have assumed that an electron is removed from oxalate in the step corresponding to k_3 to give a radical intermediate that undergoes decarboxylation. We note, however, that it is not known whether oxygen addition occurs before or after oxalate binding, and the identity of the active redox couple is still under investigation. These questions cannot be resolved on the basis of these isotope effect studies. Since, on the basis of the pH dependence of the steady-state parameters, the monoprotonated form of oxalate is the substrate, our analysis is complicated by whether (i) the protonated carboxylic acid gives rise to CO_2 or formate in the OxDC-catalyzed reaction and (ii) removal of the proton occurs in the first (k_3) or second (k_5) step of the minimal mechanism.

The equation for the effects of isotopic substitution in our minimal mechanism (eq 4), allowing for isotope effects on k_3, k_4, and k_5, can be shown to be

$$^{x}(V/K) = \frac{^{x}K_{\text{eq3}}{}^{x}k_5 + {}^{x}k_3\left(\frac{k_5}{k_4}\right) + \frac{k_3k_5}{k_2k_4}}{1 + \left(\frac{k_5}{k_4}\right)\left(1 + \frac{k_3}{k_2}\right)} \quad (5)$$

in which $x = 13$ or 18 for a ^{13}C or ^{18}O IE, respectively.

At pH 5.7, where oxalate exists almost completely as a dianion, protonation of the substrate must take place to yield the monoanion. The simplest assumption is that formation of monoprotonated oxalate occurs prior to binding, although this has not been experimentally established. In this case, ^{18}O will be enriched in the protonated carboxyl group of the substrate by 2%, so that $^{18}(V/K)$ IE at the protonated end of the molecule must be multiplied by 0.98. This then raises the question of whether the carboxylic acid moiety becomes formate or CO_2 when the substrate is bound within the OxDC active site. In all cases, given the minimal kinetic mechanism shown above (eq 4), when we assumed (i) that the oxalate carboxyl group giving rise to *formate* was initially protonated and (ii) a hydrogen atom was removed prior to decarboxylation (k_3), we could not get a reasonable fit of the experimental data to eq 5 for all of the four observed heavy-atom IEs. In a similar manner, we could not derive a consistent model at pH 5.7 assuming that the protonated substrate carboxyl ending up as CO_2 was deprotonated in the same step as decarboxylation (k_5). In contrast, the assumption that the proton was removed from this group in a step (k_3) prior to C−C bond cleavage (k_5) gave a model consistent with experimental observations (vide infra). These two conclusions were also necessary for our efforts to model the isotope effects at pH 4.2, although reproducing the data at this pH required the introduction of an external commitment.

Given these conclusions, our analysis starts by assuming that the ^{13}C IE on decarboxylation to give CO_2 is 1.04, which is an average value for such reactions,[25a,38] and that k_3/k_2 is small at pH 5.7. Under these conditions, eq 5 can be rewritten as

$$\frac{1.04 + (k_5/k_4)}{1 + (k_5/k_4)} = 1.008 \quad (6)$$

In obtaining this equation, we set the values of $^{13}K_{\text{eq3}}$ and $^{13}k_3$ to unity because proton removal from the carboxylic acid proceeds with a negligible ^{13}C isotope effect.[40] Solving eq 6 gives $k_5/k_4 = 4$, indicating that decarboxylation is 4-fold more likely to occur from the oxalate radical than the back reaction to regenerate the substrate.

Turning to the ^{18}O isotope effect at the carboxyl that becomes CO_2, $^{18}(V/K)$ must be first multiplied by 0.98 to correct for the protonated carboxyl being the initial form of the substrate. $^{18}K_{\text{eq3}}$ will then be 1.02, as a result of proton removal in the first step. Our fractionation factor calculations give an estimate of 0.967 for $^{18}K_{\text{eq5}}$ and we therefore set $^{18}k_5 = 0.983$, midway between unity and $^{18}K_{\text{eq5}}$. Assuming that k_5/k_4 is 4 and k_3/k_2 is small, as before, allows eq 5 to be written as

(38) In this analysis, we note that ^{13}C IEs on decarboxylation reactions are usually 4−5% when the heavy atom is located in the carboxylate group that is undergoing reaction. This relatively large effect arises due to the requirement that the carbon must move to become collinear with the two oxygen atoms as the reaction proceeds to yield CO_2. Assuming a slightly different value will modify the derived ratios to a small extent (when ^{13}C IE = 1.05, k_5/k_4 = 5.25) but not the overall conclusions of these experiments. In the case of carbons that are adjacent to the carboxylate group being lost from the molecule, the ^{13}C IE is decreased since these atoms undergo less motion in proceeding to the transition state for the decarboxylation step. We therefore employ a value of 1.03 in the analysis for the carbon of the substrate that becomes incorporated into formate during the OxDC-catalyzed reaction. Support for our choice of this ^{13}C IE value (3%) is provided by experiments on the oxidative decarboxylation of malate by malic enzyme (ref 39).

(39) (a) Edens, W. A.; Urbauer, J. L.; Cleland, W. W. *Biochemistry* **1997**, *36*, 1141−1147. (b) Grissom, C. B.; Cleland, W. W. *Biochemistry* **1985**, *24*, 944−948.

(40) Bayles, J. W.; Bron, J.; Paul, S. O. *J. Chem. Soc., Faraday Trans. 1* **1976**, 1546−1552.

$$\frac{0.98[(1.02)(0.983) + 4^{18}k_3]}{1+4} = 0.993 \qquad (7)$$

From eq 7, $^{18}k_3 = 1.0159$, which is a reasonable value for the deprotonation step.

For the isotope effects at the carboxylate group of oxalate that becomes formate, we can employ eq 5 to calculate $^{13}K_{eq3}$, assuming that (i) $^{13}k_5$ is 1.03, a typical value for decarboxylation,[38] and (ii) $^{13}k_3$ is midway between $^{13}K_{eq3}$ and unity. With this value, eq 5 becomes

$$\frac{1.03^{13}K_{eq3} + 4[(^{13}K_{eq3} + 1)/2]}{1+4} = 1.019 \qquad (8)$$

Solving eq 8, we find $^{13}K_{eq3} = 1.0215$, which when divided into the fractionation factor of oxalate gives 0.963, corresponding to a C−O bond order of the oxalate radical of 1.16 (Figure 2). Assuming $^{18}k_5 = 1.003$ to model the loss of C−C−O bending modes in the formate radical anion allows us to perform a similar calculation for the ^{18}O IE at this end of the molecule, since eq 5 takes the form

$$\frac{1.003^{18}K_{eq3} + 4[(^{18}K_{eq3} + 1)/2]}{1+4} = 1.01 \qquad (9)$$

From eq 9, $^{18}K_{eq3} = 1.0157$, which when divided into the fractionation factor of oxalate gives 0.9524, corresponding to a bond order of 1.14 for the C−O bonds at this end of the oxalate radical (Figure 2), in good agreement with the value of 1.16 computed on the basis of the ^{13}C IE. We will take 1.15 as an average value for the C−O bond order, which implies that the structure of the oxalate radical is a hybrid of two resonance forms, I and II, in a ratio of 70:30.

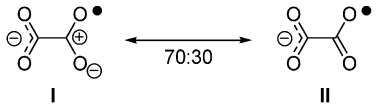

The partial positive charge on the carbon going to formate likely facilitates the decarboxylation of the radical (Scheme 2). Hydrogen transfer to the formate radical anion, formed by loss of CO_2, then yields formate, which is subsequently released from the enzyme.

At pH 4.2, oxalate is half protonated to the active monoanion form, and the small heavy-atom IEs observed at this pH (Table 1) suggest that k_3/k_2 is no longer negligible. Thus we can repeat our calculations and attempt to determine k_3/k_2 at pH 4.2. At the carboxyl end of oxalate that becomes CO_2, substitution of the observed ^{13}C IE into eq 5 gives

$$\frac{1.04 + 4\left(1 + \frac{k_3}{k_2}\right)}{1 + 4\left(1 + \frac{k_3}{k_2}\right)} = 1.005 \qquad (10)$$

Solving eq 10 gives $k_3/k_2 = 0.75$, and hence oxalate more often dissociates from the enzyme than proceeds to products. For the ^{18}O IE, we multiply the equation by 0.99, rather than by 0.98, since half of the substrate is monoprotonated, to give

$$\frac{0.99\left[(1.02)(0.983) + 4(1.0159) + 4\left(\frac{k_3}{k_2}\right)\right]}{1 + 4\left(1 + \frac{k_3}{k_2}\right)} = 0.998 \qquad (11)$$

This equation then gives $k_3/k_2 = 0.81$, a value similar to that computed on the basis of the ^{13}C IE above. Since the ^{13}C IE is better determined than the ^{18}O IE at pH 4.2, we will use $k_3/k_2 = 0.75$ in subsequent calculations.

Using the values computed for $^{13}K_{eq3}$, $^{13}k_3$, $^{13}k_5$, k_3/k_2, and k_5/k_4 from our observed isotope effects for the minimal mechanism (eq 4), we could calculate $^{13}(V/K)$ at pH 4.2 for the carboxyl group at the end of oxalate that becomes formate. Substitution into eq 5 gives

$$\frac{(1.03)(1.0215) + 4(1.0108) + 3}{1+4+3} = 1.012 = {}^{13}(V/K)$$

which is in good agreement with the experimental value of 1.015. For the ^{18}O isotope effect, we must multiply by 1.01 to correct for the half-protonation of the substrate, and so eq 5 becomes

$$\frac{1.01[(1.003)(1.0157) + 4(1.0078) + 3]}{1+4+3} = 1.016 = {}^{18}(V/K)$$

which compares with the experimental value of 1.011. While the agreement between theory and experiments is not perfect in this case, the kinetic model for OxDC-catalyzed decarboxylation does fit the experimental data in a reasonable fashion.

Molecular Mechanism for the Enzymatic Reaction of OxDC. The catalytic mechanism of OxDC proposed here invokes the participation of a substrate-based radical in order to facilitate cleavage of the C−C bond. This hypothesis is supported by (i) the dependence of OxDC activity on catalytic levels of dioxygen,[12,14] (ii) the presence of manganese, which can abstract an electron from bound substrate, in the active site(s) of the enzyme,[13,14] (iii) the absence of other cofactors in the OxDC structure,[15] and (iv) no net redox change between substrate and products. OxDC cannot be regarded as an oxidase because only 0.2% H_2O_2 is formed during the enzyme-catalyzed reaction,[12,14] presumably as a result of an unproductive side reaction. The involvement of thiyl radicals, as in the mechanism of pyruvate formate lyase, is also precluded by the absence of cysteine residues in the active site(s) of *B. subtilis* OxDC and the fact that oxalate is not susceptible to nucleophilic attack by sulfur.

Our observed isotope effects rule out any mechanism for OxDC that does not include an isotope-sensitive, reversible step prior to decarboxylation. The normal IEs found for both carbon and oxygen also limit the possible number of mechanisms employed by the enzyme. One proposal, however, that accounts for the observed ^{13}C or ^{18}O IEs and is consistent with the crystal structure of the OxDC active site,[15] involves a bound oxalate radical (Scheme 2). Since we have established that CO_2 is

Scheme 2. Hypothetical Mechanism of *B. subtilis* OxDC-Catalyzed C−C Bond Cleavage Showing Possible Roles of Arg-270 and Glu-333[a]

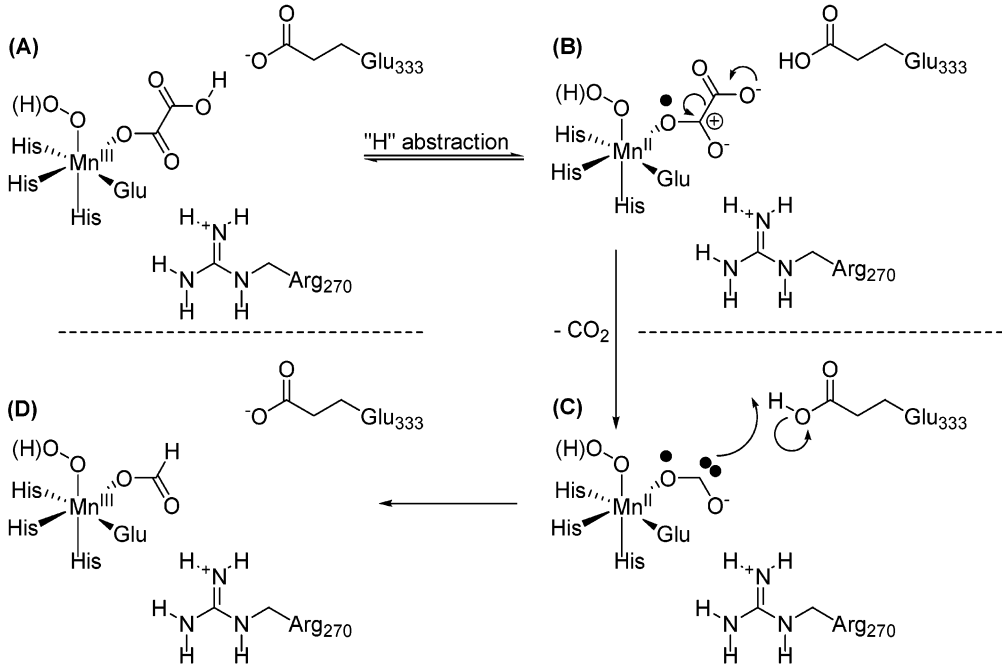

[a] (A) Monoprotonated oxalate and oxygen bind to the Mn metal center. The oxidation state of Mn in this and succeeding structures is hypothetical and remains to be determined. (B) Glu-333 acts as a general base to remove a proton while electron transfer takes place to generate an oxygen-centered radical. Arg-270 polarizes the C−O bond of the substrate, building up positive charge on the carbon atom, thereby facilitating heterolytic cleavage of the C−C bond to give CO_2. (C) Representation of the product of decarboxylation that is consistent with the model for the C−O bond orders derived from the measured KIEs. This species is a resonance form of the formate radical anion. Coupled proton−electron transfer, possibly involving Glu-333, then yields formate.

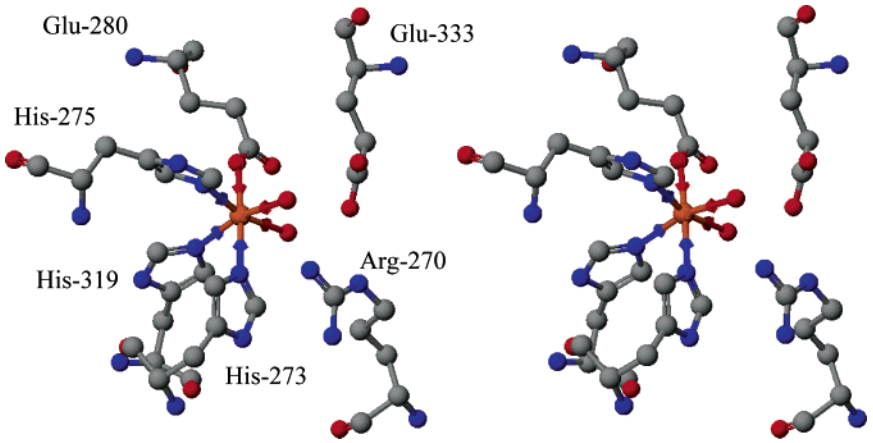

Figure 3. Stereo representation of the C-terminal active site of *B. subtilis* OxDC. Conserved residues that may play a role in catalyzing C−C bond cleavage are shown adjacent to the Mn center in the active site. Two water molecules, which are presumably displaced on substrate binding, coordinate the Mn. All atoms are shown at their crystallographic coordinates.[15] Hydrogens have been omitted for clarity. Key: C, gray; N, blue; O, red; Mn, orange.

formed from the protonated end of bound oxalate, our mechanism implies, on the basis of simple electrostatic considerations, that the carboxylate anion of the substrate, rather than the carboxylic acid moiety, would be directly attached to the metal ion. Here we present this mechanism, with the assumption that Mn(II) and Mn(III) are the redox-active forms of the metal during catalysis, although the actual catalytic species remains to be demonstrated by spectroscopic studies. In our mechanism, the reversible slow step required by the IE results presumably corresponds to the oxidative transfer of a single electron from oxalate to a Mn(III) hydroperoxide, or superoxide complex, accompanied by proton transfer from the protonated substrate to a nearby residue. On the basis of the OxDC crystal structure, the side chain of Glu-333 could function as the general base in the deprotonation reaction due to its proximity to the bound substrate (Figure 3).[15] An important consequence of such a model would be that only the C-terminal, Mn-binding site would be catalytically active given the apparent absence of a suitable general base in the other, N-terminal site. The proton transfer at this step is supported by not only the IE studies but also the fact that oxalate dianion is easier to oxidize (~0.7 eV) than the mononanion.[41] The IE measured here for formation of formate appears to be largely an equilibrium one. Thus, the oxalate radical formally has an empty p orbital on carbon and a single

(41) Isse, A. A.; Gennaro, A.; Maran, F. *Acta Chem. Scand.* **1999**, *53*, 1013−1022.

odd electron in a p orbital on oxygen, which may delocalize directly onto the p orbital of the nearby oxygen, forming a three-electron π bond (Scheme 2B).[42] Removing an electron therefore reduces the bond order between carbon and oxygen, causing the normal ^{13}C and ^{18}O IEs observed for formation of formate. We note that Arg-270 (Figure 3) might play a role in polarizing the C−O bond in the Mn-bound, radical intermediate through an electrostatic interaction. Decarboxylation and C−C bond cleavage in a second step, facilitated by the partial positive charge on the carbon that will become formate, then results in formation of a formate radical anion having a negative charge at the carbon atom (Scheme 2C). This step, which is faster than reversal of the first one, is consistent with the observation of the small normal ^{13}C IE that is measured for CO_2. In the final steps of the OxDC-catalyzed reaction, the formate radical anion acquires a proton, possibly from residue Glu-333, and an electron from the enzyme-bound metal ion to yield the product formate.

A key conclusion of these IE studies is that the radical used to initiate decarboxylation is not located on the carboxyl group that eventually forms CO_2. In addition, our proposal for the OxDC-catalyzed reaction (Scheme 2) suggests that decarboxylation involves heterolytic breakdown of the C−C bond. Both of these features contrast with the chemical mechanisms determined for radical-mediated decarboxylations, such as the Kolbe[43] or Hunsdiecker[44] reactions, in which a carboxyl radical intermediate loses CO_2 by homolytic C−C bond cleavage to give an alkyl radical that can itself undergo further reaction. The large drop in bond order determined for the substrate C−O bonds of the carboxylate that forms formate in the OxDC-catalyzed reaction, however, is clear evidence that the radical initiating decarboxylation cannot be present on the carboxylate that is converted to CO_2.

Acknowledgment. We thank Drs. Tadhg Begley and Steven Ealick (Cornell University) for useful discussions and X-ray coordinate data prior to publication. The National Institutes of Health (Grants DK53556 and GM18938) and the Oxalosis and Hyperoxaluria Foundation (N.G.J.R.) provided generous financial support for this work. Technical support for DNA sequencing was provided by the Interdisciplinary Center for Biotechnology Research at the University of Florida.

Appendix

Although oxalate (A) is symmetrical, the two ends of the molecule when bound to OxDC are not equivalent and therefore yield different products, formate (B) and CO_2 (C). If the heavy isotope is at the end of the substrate that becomes formate (shown as *A below), this gives an IE of k_b*. Equally, if the heavy isotope is at the end of the substrate that becomes CO_2 (shown as A* below), this gives an IE of k_c*:

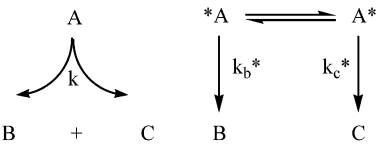

If we define A = [oxalate], B = [formate], and C = [CO_2], we can write

$$A + B = A_0 \qquad B = C \qquad A^* + B^* + C^* = A_0^*$$

$$R_0 = A_0^*/A_0 \qquad f = B/A_0 = C/A_0 \qquad 1 - f = (A_0 - B)/A_0$$

The conversion of oxalate to products is described by the following differential equation:

$$-dA/dt = kA = dB/dt = dC/dt \tag{A1}$$

and the effect of isotopic substitution leads to

$$dB^*/dt = (1/2)k_b^*A^* \qquad \text{and} \qquad dC^*/dt = (1/2)k_c^*A^* \tag{A2}$$

Hence, $dC^*/dB^* = k_c^*/k_b^*$, which integrates to

$$C^*/B^* = k_c^*/k_b^* = x \tag{A3}$$

From eq A3, it is clear that x remains constant during oxalate breakdown and is therefore best determined by letting the reaction go to completion. In this case, $x = R_c/R_b$, where R_c and R_b are the mass ratios in C and B, respectively.

Case I: Heavy Atom Isotope Effects by Analysis of Residual Oxalate. The effect of heavy atom substitution in the carboxyl group that becomes formate is described by the following differential equation:

$$dB^*/dB = (1/2)\, k_b^*A^*/(kA)$$

which, by use of the relationships given above, can be rearranged to yield

$$\frac{dB^*}{A^*} = \left[\frac{(1/2)k_b^*}{k}\right]\left[\frac{dB}{(A_0 - B)}\right] \tag{A4}$$

Using the fact that $A^* = A_0^* - B^* - C^* = A_0^* - B^*(1 + x)$, we can write

$$\frac{dB^*}{A_0^* - B^*(1 + x)} = \left[\frac{(1/2)k_b^*}{k}\right]\left(\frac{dB}{A_0 - B}\right)$$

which integrates to give

$$\left(\frac{1}{1 + x}\right) \ln \frac{[A_0^* - B^*(1 + x)]}{A_0^*} = \frac{(1/2)\, k_b^*}{k} \ln (1 - f) \tag{A5}$$

If we let R_s and R_0 be the mass ratios in the residual and initial oxalate, respectively, then

$$R_s = \frac{A_0^* - B^*(1 + x)}{(A_0 - B)} \tag{A6}$$

$$\frac{R_s}{R_0} = \frac{[A_0^* - B^*(1 + x)]}{(A_0 - B)}\left(\frac{A_0}{A_0^*}\right) = \left[\frac{A_0^* - B^*(1 + x)}{A_0^*}\right]\left(\frac{1}{1 - f}\right) \tag{A7}$$

(42) (a) McBride, J. M.; Merrill, R. A. *J. Am. Chem. Soc.* **1980**, *102*, 1723−1725. (b) Rauk, A.; Dake, Y.; Armstrong, D. A. *J. Am. Chem. Soc.* **1984**, *116*, 8222−8228. (c) Jonsson, M.; Wayner, D. D.; Lusztyk, J. *J. Phys. Chem.* **1996**, *100*, 17539−17543.

(43) (a) Schäfer, H. J. *Angew. Chem., Int. Ed. Engl.* **1981**, *20*, 911−934. (b) Vijh, A. K.; Conway, B. E. *Chem. Rev.* **1967**, *67*, 623−644. (c) Kraeutler, B.; Jaeger, C. D.; Bard, A. J. *J. Am. Chem. Soc.* **1978**, *100*, 4903−4905.

(44) (a) Johnson, R. G.; Ingham, R. K. *Chem. Rev.* **1956**, *56*, 219−269. (b) Bunce, N. J.; Murray, N. G. *Tetrahedron* **1971**, *27*, 5323−5335.

Combining eqs A5−A7, we obtain

$$\left(\frac{1}{1+x}\right)\ln\left[(1-f)\left(\frac{R_s}{R_0}\right)\right]=\frac{(1/2)k_b^*}{k}\ln(1-f) \quad \text{(A8)}$$

and so

$$\text{apparent isotope effect}=\frac{2k}{(1+x)k_b^*}=\frac{\ln(1-f)}{\ln\left[(1-f)\left(\frac{R_s}{R_0}\right)\right]}$$

Use of eq A3 to replace k_b^* in eq A8 then gives

$$\text{apparent isotope effect}=\frac{2xk}{(1+x)k_c^*} \quad \text{(A9)}$$

Thus

$$\frac{k}{k_b^*}=\frac{(1+x)}{2}(\text{apparent isotope effect}) \quad (3)$$

$$\frac{k}{k_c^*}=\frac{(1+x)}{2x}(\text{apparent isotope effect}) \quad (2)$$

The value of x, needed to obtain the heavy atom isotope effects, is determined as described above.

Case II: Heavy Atom Isotope Effects by Analysis of Formate and CO_2. If we define A = [oxalate], B = [formate], and $C = [CO_2]$, we can write

$$A_0^* - B_0^*(1+x) = A_0^* - B^* - C^*$$

$$R_0 = A_0^*/A_0 \qquad R_b = B^*/B \qquad R_c = C^*/C$$

Therefore

$$f(R_b/R_0) = (B/A_0)(B^*/B)(A_0/A_0^*) = B^*/A_0^* \quad \text{and}$$

$$f(R_c/R_0) = C^*/A_0^*$$

Note that R_0 in these expressions is for the whole molecule. Then

$$\frac{A_0^* - B^* - C^*}{A_0^*} = 1 - \frac{f(R_b + R_c)}{R_0} \quad \text{(A10)}$$

and hence we obtain

$$\text{apparent isotope effect} = \frac{\ln(1-f)}{\ln\left[1 - f\dfrac{(R_b + R_c)}{R_0}\right]} \quad \text{(A11)}$$

JA0286977